Classical Trajectory Simulations of Photoionization Dynamics of Tryptophan: Intramolecular Energy Flow, Hydrogen-Transfer Processes and Conformational Transitions†

Dorit Shemesh‡ and R. Benny Gerber*,‡,§

Department of Physical Chemistry and the Fritz Haber Research Center, The Hebrew University, Jerusalem 91904, Israel, and Department of Chemistry, University of California, Irvine, California 92697

Received: December 6, 2005; In Final Form: January 15, 2006

One-photon and two-photon ionization dynamics of tryptophan is studied by classical trajectory simulations using the semiempirical parametric method number 3 (PM3) potential surface in "on the fly" calculations. The tryptophan conformer is assumed to be in the vibrational ground state prior to ionization. Initial conditions for the trajectories are weighted according to the Wigner distribution function computed for that state. Vertical ionization in the spirit of the classical Franck−Condon principle is assumed. For the two-photon ionization process the ionization is assumed to go resonantively through the first excited state. Most trajectories are computed, and the analysis is carried out for the first 10 ps. A range of interesting effects are observed. The main findings are as follows: (1) Multiple conformational transitions are observed in most of the trajectories within the ultrafast duration of 10 ps. (2) Hydrogen transfer from the carboxyl group to the amino group and back has been observed. A zwitterion is formed as a transient state. (3) Two new isomers are formed during the dynamics, which have apparently not been previously observed. (4) Fast energy flow between the ring modes and the amino acid backbone is observed for both one- and two-photon ionization. However, the effective vibrational temperatures only approach the same value after 90 ps. The conformation transition dynamics, the proton-transfer processes and the vibrational energy flow are discussed and analyzed.

I. Introduction

The mechanism and dynamics of photoionization of biological molecules are of considerable intrinsic interest and may have potential applications, especially in mass spectrometry. Ionization, carried out by several possible processes,[1−4] is obviously a central aspect of mass spectrometry. At the same time, mass spectrometry has already developed into a major tool in the study and characterization of biological molecules, from small to very large.[5−23] Little is currently known on the dynamical processes that take place upon photoionization of biological molecules. The present article aims at exploring this topic. We chose to focus on single-photon ionization and two-photon ionization in this study,

The channels that open up upon ionization are many and include internal flow and redistribution of the vibrational energy between the modes, conformational transitions of the nascent ion, transfer of hydrogen within the ion,[24,25] and fragmentation of the ion.[21,26,27] The study presented here focuses mostly on the three types of processes: intramolecular vibrational energy redistribution (IVR), transitions between different conformers and internal proton transfer. These seem to be the fastest and most efficient dynamical processes in such systems. However, other chemical processes that involve bond breaking or shifting and require much longer time scales depend ultimately on the outcome of the IVR and conformational transition events. It is important to know whether a statistical distribution of vibrational energy is indeed obtained and on which time scale it is reached. The question is, how long after the ionization is a vibrational distribution compatible with Rice−Ramsperger−Kassel−Marcus (RRKM) theory obtained? The time scale that will be explored here is short, only 10 ps, but it is useful to know if the system approaches a statistical distribution within this time scale. If not, characterization of the patterns of vibrational energy flow is of considerable interest. The issue of conformational transitions is likewise important: Which conformers are populated following ionization, and on which time scale does this take place? This issue is often discussed qualitatively in mass spectrometry, but it seems that it was not studied quantitatively by dynamics simulations. Another interesting question is whether some fragmentation events can take place already on the short time scale studied here. Clearly, the yield for such processes on this short time scale is expected to be very low, but it is interesting to explore if the event is not too rare to be seen for some of the trajectories in the set (and hopefully to be measured experimentally). For the set of trajectories used, no fragmentation events are found. In summary, the present paper explores the dynamical evolution of the system after ionization, using classical trajectory simulations and a semiempirical potential surface, the choice of which will be discussed later. The one- and two-photon ionization of tryptophan has been studied in this work. Tryptophan is an aromatic amino acid, containing an indole group as the chromophore. Tryptophan has been well characterized by experiments and calculations,[21,28−44] in particular, the neutral conformers existing in a supersonic beam and in matrix have

† Part of the "Chava Lifshitz Memorial Issue".

* To whom correspondence should be addressed. E-mail: benny@fh.huji.ac.il.

‡ The Hebrew University.

§ University of California.

10.1021/jp0570869 CCC: $33.50 © 2006 American Chemical Society
Published on Web 02/15/2006

been identified using spectroscopy. The excited states of tryptophan are well-known.[30,37] In the gas phase, the lowest lying excited singlet state is denoted by ^1L_b and the second excited singlet state by ^1L_a.[30,37] The mass spectra of tryptophan have been recorded by different groups.[21,30−36,38] Still, there is no available experimental data on the ionic surface as, for example, stable ionic conformers. We also note that due to the open-shell structure of the radical ion produced, theoretical calculations of the potential surface are difficult. There are so far no computational studies related to the ionic potential energy surface.

The structure of the article is as follows. Section II presents the methodology, section III presents the results and section IV brings concluding remarks.

II. Methodology

a. Potential Energy Surface. Biological molecules are most often studied using empirical force fields such as AMBER,[45,46] OPLS,[47,48] MMFF94.[49,50] The advantages of these force fields are that they are simple to use, computationally fast and give adequate results for neutral molecules. However, these force fields are inapplicable for many ionic molecules, because they were not parametrized for such cases. This is certainly the case here, because the system is a radical ion.

A more accurate approach is to use ab initio potentials, but these are computationally expensive, even for biological molecules of modest size. In dynamical simulations the potential energy is evaluated thousands of times along the trajectories. This operation is the main computational effort in such simulations, and using ab initio potentials would be very time-consuming. Such ab initio simulations would be limited to only very short time scales and for the smallest systems.

Therefore, we use in this study PM3 semiempirical electronic structure theory.[51,52] PM3 is one of several modified semiempirical NDDO approximation (neglect of diatomic differential overlap) methods.[53] Rather than performing a calculation of all the integrals required in the formation of the Fock matrix, three- and four-center integrals are neglected in PM3, and one-center, two-electron integrals are parametrized. Obviously, PM3 is closer to ab initio methods than to empirical force field. Additionally, PM3 has recently been applied to calculations of small proteins.[54−56] It is not known if PM3 possesses the capability of correctly describing bond breaking for radical ions. Another problem that may arise is the Hartree−Fock instability and possible degeneracy for open shell systems. Recently, a method has been developed in our group, which improves PM3 potential energy surfaces.[57] This method modifies PM3 potential surfaces, by fitting them to ab initio potentials at the harmonic level. The modified PM3 potential has been tested for glycine, alanine and proline by calculating the anharmonic frequencies using the vibrational self-consistent field (VSCF) and correlation-corrected vibrational self-consistent field (CC-VSCF)[58,59] method and comparing them to experimental data. The computed anharmonic frequencies are in very good agreement with spectroscopic experiments for these three amino acids. Unfortunately, this potential energy surface is currently unavailable for dynamical simulations. It is also not quite sure if it is applicable to dynamical simulation, because the improvement is done only for the region around the equilibrium geometry. The simulations presented here were carried out with standard PM3.

All calculations here were performed using the electronic structure package GAMESS.[60] The relevant conformers were optimized using PM3 semiempirical electronic structure theory on the neutral surface. For tryptophan the global minimum[42] was computed and optimized by PM3. The second derivative (Hessian) matrix was calculated to ensure that the stationary point is indeed a minimum. Harmonic normal-mode analysis was performed on this geometry. Initial coordinates for tryptophan for simulating the single-photon ionization were chosen by the following procedure: Each mode has been distorted from equilibrium. For each mode 16 different positions were chosen and the Wigner distribution for these geometries was calculated. By this procedure, 1200 initial geometries were found. The excess energy of these geometries on the ionic surface (compared to a reference nearby ionic minimum) was computed and the 100 geometries with the highest excess energy were chosen as initial geometries. The selection of these particular configurations was done merely to explore the richer dynamics that takes place at high excess energies. It should be noted that the one-photon processes were modeled for a nonmonochromatic, broadband excitation.

For the two-photon ionization process of tryptophan 91 initial geometries were found by the following procedure: Simultaneously two modes were distorted from equilibrium each on a 16 points grid. A total of 710 400 geometries were found in this way.

The excitation energy of the first excited state has been measured by Levy and co-workers[30] and corresponds to 34 873 cm^{-1} (4.32 eV). The two-photon ionization mechanism is presumed to go through this state. The vertical ionization energy therefore is equal to two photons (8.64 eV). Only geometries with ionization energy of 8.64 eV were accepted. A total of 91 geometries were chosen in such a way that their ionization energy differs up to 0.001 eV from the above value. Note that most of the 710 400 geometries do not have this property and therefore are not suitable for simulating the two-photon ionization.

For each geometry in the Franck−Condon regime, single-photon ionization was modeled by vertical promotion into the ionic potential energy surface. For two-photon ionization it is assumed that the first photon promotes the system to the first excited state. Immediately, a second photon is absorbed, which leads to the desired ionization. The absorption of the two photons is assumed to happen very fast, so that the geometry does not change at all. Evidence for this is provided by the study of Kushwaha et al.[39] and Rizzo et al.[29] Kushwaha et al.[39] show in their calculations that the first excited-state geometry of tryptophan is almost equivalent to the neutral geometry. Rizzo et al.[29] show in a supersonic beam experiment that the excited state conformers of tryptophan do not interconvert during the fluorescence lifetime. Note that the initial geometry sampling for single- and two-photon ionization is different. The simulation assumes a broad band excitation for the single-photon ionization. Therefore each geometry chosen by the above procedure is suited for the simulation. In contrary, the two-photon ionization process implies that the ionization energy is exactly equal to two photons of certain energy. The assumed procedure of the two-photon ionization process goes through an excited state, which is well-known and measured experimentally. Therefore the initial geometries chosen have to fulfill this property. This leads to a small number of accepted geometries.

b. Classical Trajectory Simulations of the Dynamics. The method used for the simulation is "on the fly" molecular dynamics[61−67] that is implemented into the electronic structure program package GAMESS. Recently, studies of dynamics on the fly using quantum mechanics/molecular mechanics (QM/MM) and semiempirical potentials have been pursued by Hase

and co-workers.[68,69] Obviously, some quantum effects are expected to play a role, and these are neglected in the classical approach. Zero-point energy is probably the most important quantum effect neglected in this study. However, the excess energy is fairly high on the ionic states ($E > 0.8$ eV) and we assume the classical description should be reasonable. In "on the fly" molecular dynamics, at each time step the current potential energy is evaluated and the forces are computed. The atoms are moved according to these forces to a new position (next time step), and there again, the forces are calculated from the potential energy and the atoms are moved, and so on. A very demanding self-consistent field (SCF) convergence criterion of 10^{-11} was employed to ensure in this case accurate force calculations for the time scale of the study. The default value of 10^{-5} employed in the standard GAMESS code is not sufficiently small for the present case. Calculations with the standard value have shown that the computed trajectory contains unphysical artifacts. The reason is obvious: The more accurate the potential energy calculation, the more accurate will be the force calculations at that point. Fewer errors are then accumulated during the simulation and the calculated trajectory deviates less from the true one. Each trajectory was calculated for 10 ps with a time step of 0.1 fs (to ensure energy conservation). The ionization was modeled by vertical promotion into the ionic potential energy surface. After ionization the trajectory was propagated in time on the ionic PM3 potential energy surface (using restricted open-shell Hartree−Fock (ROHF) in the Hartree−Fock part of the code). Trajectories where the ROHF energy calculations failed to converge, or for which energy conservation was not satisfied, were rejected. Energy was considered to be conserved, when the difference between the initial total energy and the total energy (in atomic units) at the current time step was smaller than 5×10^{-5}. The analysis was all carried out for the remaining trajectories.

c. Modeling the Initial State for One- and Two-Photon Ionization. The molecule is assumed to be initially in its vibrational ground state. This is an experimentally realizable (e.g., in low temperature beam experiments), well-defined condition. For such an initial state, the classical description is quite unrealistic (classically, the system at $T = 0$ K is initially at rest at the minimum configuration, with no zero point energy), so there will be only one classical trajectory for these conditions. Classical description becomes closer to reality if the simulations are done for initial temperature $T > 0$, in fact for sufficiently high T. In summary, the ground-state vibrational wave function is appropriate for sampling the initial state. Furthermore, for this state the anharmonic corrections are modest, and a harmonic wave function seems a reasonable wave function.

To sample trajectories according to the initial state, we use the Wigner distribution function:[70]

$$W(r,p) = \left(\frac{1}{2\pi\hbar}\right)^N \int \mathrm{d}s \exp\left[\frac{is\cdot p}{\hbar}\right] \cdot \Psi^*\left(r + \frac{s}{2}\right) \Psi\left(r - \frac{s}{2}\right) \quad (1)$$

where ψ is the wave function of the state, r are the coordinates, and p are the momenta.

Each normal mode is treated as a classical harmonic oscillator in its ground vibrational state. Substitution of the harmonic oscillator wave function into the Wigner distribution gives the position and momentum distribution for an n-dimensional harmonic oscillator:

$$W(q,p) = (\pi\hbar)^{-n} \prod_{i=1}^{n} \mathrm{e}^{-p_i^2/\alpha_i} \mathrm{e}^{-k_i q_i^2/\alpha_i} \quad (2)$$

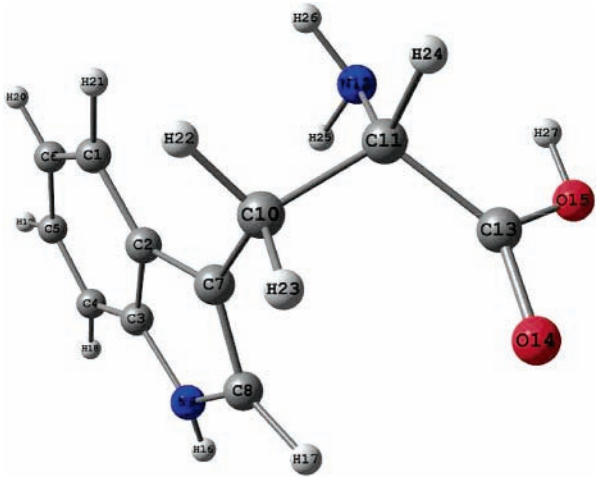

Figure 1. Global neutral minimum of tryptophan as optimized by PM3.

q_i are the normal mode coordinates, and p_i are the corresponding momenta. k_i is the force constant of the ith normal mode and α_i is related to the corresponding vibrational frequency ($\alpha_i = \hbar\omega_i$). For the excitation process, we assume in the spirit of the Franck−Condon principle, vertical promotion to the ionic state. This implies that the initial velocities are zero on the ionic surface, the configurations being those sampled for the neutral species.

III. Results and Discussion

1. Two-Photon Ionization of Tryptophan. Figure 1 shows the global neutral minimum of tryptophan as optimized by PM3. Tryptophan consists of an aromatic indole group and an amino acid backbone. The indole ring is mainly planar. Note that the distance between O14 and H17 in the global minimum is 2.81 Å. The aromatic group vibrates only very little upon ionization. The main conformational changes occur in the amino acid backbone. A large number of the trajectories show the very stable conformer with the hydrogen bond between O14 and H17. There are also other stable conformers that appear during the dynamics. One trajectory is chosen here to show the conformers accessed during the simulation. The time scale of the trajectory is 10 ps. The excess energy for this trajectory is 3.13 eV.

Figure 2 shows snapshots of the dynamics. Initially, the amino acid backbone is almost perpendicular to the plane of the indole ring. During the first picosecond the COOH group undergoes a 90° turn about the C11−C13 bond. A new hydrogen bond between oxygen O14 of the carbonyl group and hydrogen H17 of the indole ring is created. This gives rise to an especially stable conformer (named here conformer I) that is also observed in other trajectories. Figure 2 shows this conformer at $t = 1.33$ ps. There exist several conformers that also contain this hydrogen bond but differ in the arrangement of the NH_2 group and the OH group. This conformer is kinetically relatively stable. It exists in this trajectory for about 3.2 ps. During this time span the NH_2 group rotates freely about the C−N bond. Then, the whole amino acid backbone turns about the C7−C10 and breaks the hydrogen bond between the carbonyl group and the indole group. This hydrogen bond is replaced by a new hydrogen bond between the nitrogen of the NH_2 group and the same hydrogen of the indole ring. This conformer is created at about 4.52 ps. This is another kinetically stable conformer (named here conformer II) that is also observed in other trajectories. The system stays in this conformer for about 3.4 ps and then turns back to the first conformer with the hydrogen bond

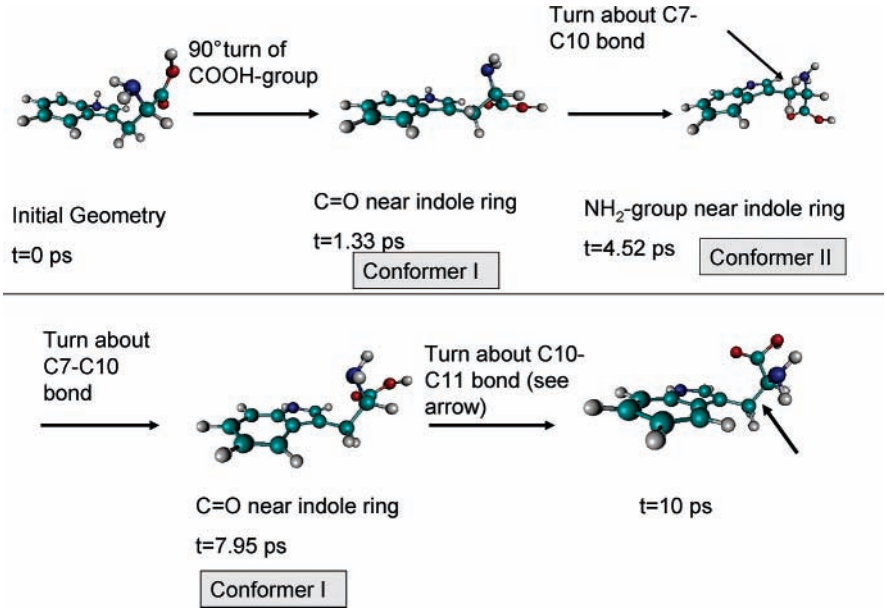

Figure 2. Snapshots of the two-photon ionization dynamics of one trajectory.

between the oxygen of the carbonyl group and the hydrogen of the indole group. At the end of the simulation this hydrogen bond again breaks apart and the amino acid backbone turns about the C10−C11 bond to give another conformer. Most of the trajectories show the creation of the two hydrogen-bonded conformers. Other conformers are also created but are not mentioned here. The time scale of their creation differs from trajectory to trajectory, and also the order of their appearance.

For this trajectory the energy flow between the ring modes and the amino acid was calculated in the following way. The kinetic energy of each normal mode in this trajectory was calculated vs time. The system was divided into a subset of normal modes located predominantly on the indole ring (39 normal modes) and a subset of modes located predominantly on the amino acid backbone. The kinetic energies of the modes related to the indole ring and of the modes related to the amino acid backbone atoms were separately summed and temperatures for the indole ring and for the amino acid backbone subsets were defined in terms of the corresponding kinetic energies. The temperature of each part at time t is thus

$$T(t) = \frac{2E_{\mathrm{kin}}(t)}{k} \tag{7}$$

where k is the Boltzmann factor and $E_{\mathrm{kin}}(t)$ is the kinetic energy of a single normal mode within the part at time t. The high frequency fluctuations of the effective temperatures were averaged over time. The effective temperatures versus time are plotted in Figure 3. From the figure it can be seen that initially the amino acid is much hotter than the indole ring. The amino acid backbone undergoes conformational changes in the first picosecond; therefore the effective temperature changes much. Still after creation of the first conformer there are still large fluctuations in the effective energy of the amino acid backbone. Although a stable conformer is created, there are still movements in the molecule, like, for example, the rotation of the NH_2-group. The creation of the second conformer leads to smaller changes in the effective temperature. The reason is the following one: Only this conformer vibrates, and therefore the effective temperature does not change too much. The conformational changes in the last picoseconds involve large fluctuations in

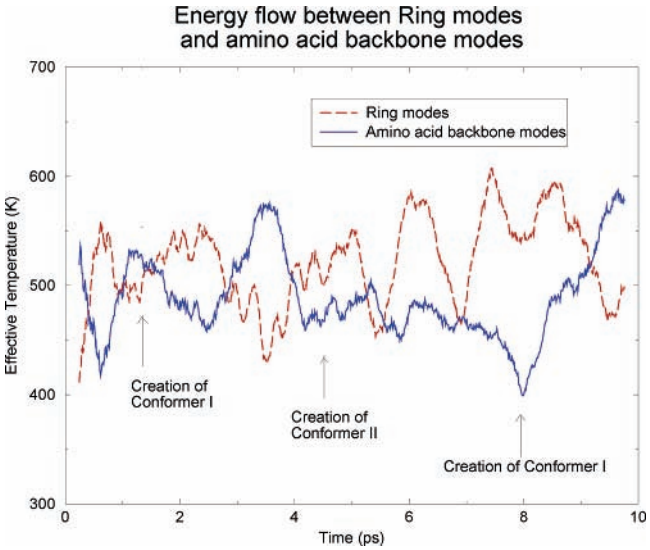

Figure 3. Effective temperature of the ring modes and the amino acid backbone modes of the trajectory drawn in Figure 3.

the effective temperature. The indole ring is a very stable structure and therefore does not change too much as it vibrates. But still, there is an extensive energy flow into and out of the indole ring. During the entire simulation time, the energy fluctuates about some common temperature, but until the end there is no full equilibrium to this temperature. The large fluctuations persist until the end. One has to keep in mind that this is only an example of one trajectory. Equilibration can still be reached if one looks at the average energy flow of all the trajectories. Therefore, the same procedure has been done for all trajectories (there are 72 trajectories that reached 10 ps). The effective temperatures were averaged using the statistical weight from the Wigner distribution for each trajectory. The result is shown in Figure 4. Also here it can be seen that the energy flow between the ring modes and the amino acid is fast. There seems to be no bottleneck between these two parts. After 10 ps the system reaches equilibrium between the two parts. But, a closer look at the energy flow between the each pair of normal mode may still reveal that some modes do not exchange energy

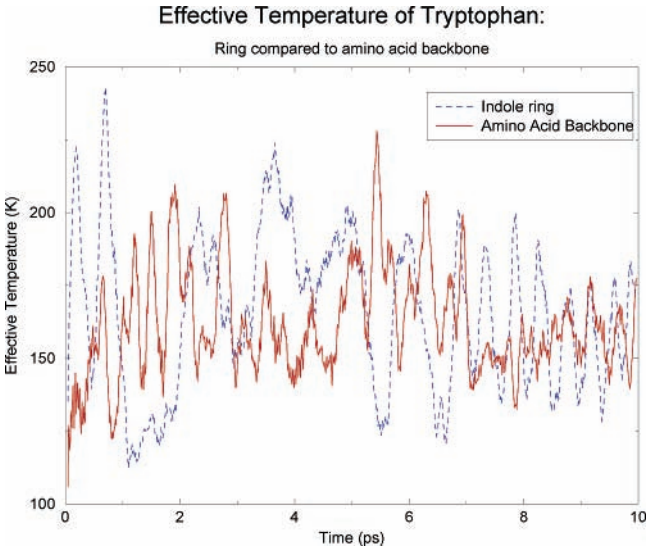

Figure 4. Effective temperature of the ring modes and the amino acid backbone modes of the two-photon ionization averaged over all trajectories up to 10 ps.

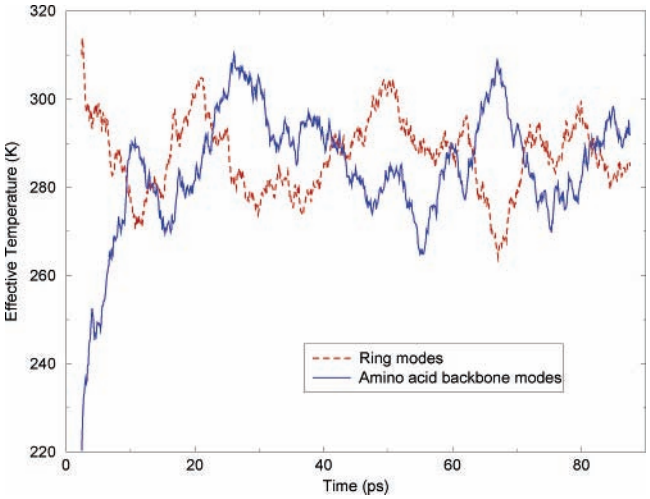

Figure 5. Effective temperature of the ring modes and the amino acid backbone modes of the two-photon ionization averaged over all trajectories up to 90 ps.

with some other modes. The approach of dividing the molecule into two parts ignores this type of possible bottlenecks.

The effective temperature flow between ring modes and amino acid backbone has been calculated from 29 trajectories up to 90 ps. The result is shown in Figure 5. As can be seen, there is an intensive energy exchange between the ring modes and the amino acid backbone, which persists until the end of the simulation. The system does not reach equilibration but seems to approach it closely. Note that the number of trajectories used here is quite small (only 29). An increase of the number of trajectories could lead to a more accurate description. However, our impression is that the results will not change dramatically. A tentative explanation of this figure is therefore that IVR (intramolecular vibrational energy redistribution) is not as fast as assumed. Significant vibrational nonequilibrium effects remain up to 90 ps, even for these conditions of high energy.

In summary, the two-photon ionization of tryptophan leads to conformational changes. This gives insight as to which different conformers are populated during a mass spectrometric experiment. Obviously, for longer time scales, more conformers

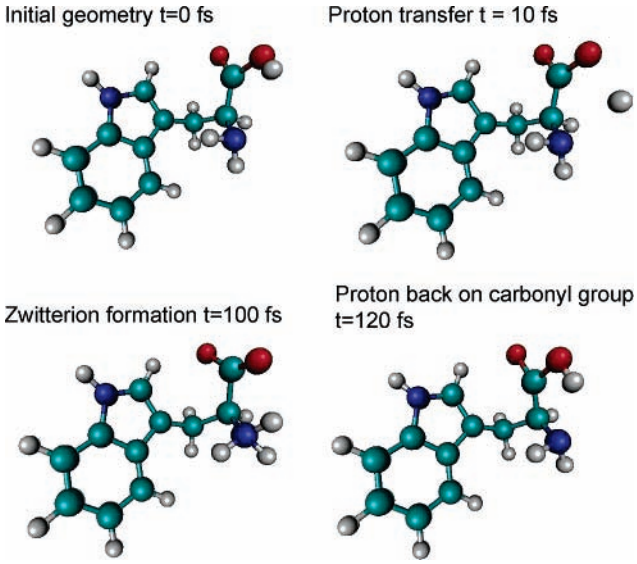

Figure 6. Snapshots of the one-photon ionization dynamics of tryptophan: proton transfer, creation of the zwitterion and proton-transfer back.

may became populated. The trajectories calculated here only show conformational changes as seen in the above case, no isomerization or fragmentation is found for the two-photon ionization process. This may be due to the fact that the energy is unsufficient to this changes in the time scales studied.

2. One-Photon Ionization of Tryptophan. Most of the trajectories here also show the same conformational transitions described in example above. Therefore, only special conformers will be described in this part. This trajectories are mostly characterized by a high excess energy.

(a) Hydrogen Transfer. Two trajectories out of 94 show hydrogen transfer from the hydroxyl group to the amino group and creation of a zwitterion. In both trajectories the OH stretch is distorted initially from equilibrium. One of them is chosen here to show the dynamical evolution of the zwitterion creation. Snapshots of the dynamics can be seen in Figure 6. In this trajectory the OH-stretch mode (frequency: 3860.27 cm^{-1}) is distorted initially to −30.1609 au. The starting geometry is drawn in Figure 6. The excess energy for this trajectory is 7.2 eV. The OH-stretch motion leads to the breaking of the OH bond at 10 fs. The proton then jumps to the amino group at 100 fs and creates and a zwitterion. The lifetime of this zwitterion is very short. At 120 fs the proton jumps back to the oxygen and stays there until the end of the simulation.

(b) Creation of New Isomer. One of the trajectories shows the creation of a new isomer. In this trajectory, the NH stretch of the indole ring (frequency: 3465.36 cm^{-1}) was distorted to $q = 31.833\ 11$ au. The excess energy for this trajectory is 6.3 eV. Snapshots of the dynamical evolution of the new isomer can be seen in Figure 7. In the initial geometry the amino acid backbone is almost perpendicular to the indole ring. After 0.71 ps the COOH turns, such that the carbonyl group is now near H17 of the indole group (conformer I). Then after about 2 ps, the system switches to conformer II where the amino group is near the indole group. This conformer remains stable for about 3 ps. At the end of this time span the amino acid backbone turns about the C7−C10 bond. Also the COOH group rotates about 180° back and forth. The resulting conformer can be seen in Figure 7 ($t = 5.81$ ps). This conformer overcomes another turn about the C7−C10 bond with half a rotation of the COOH group. Note that the amino acid backbone has rotated a full rotation about the C7−C10 bond from the beginning until 6.31

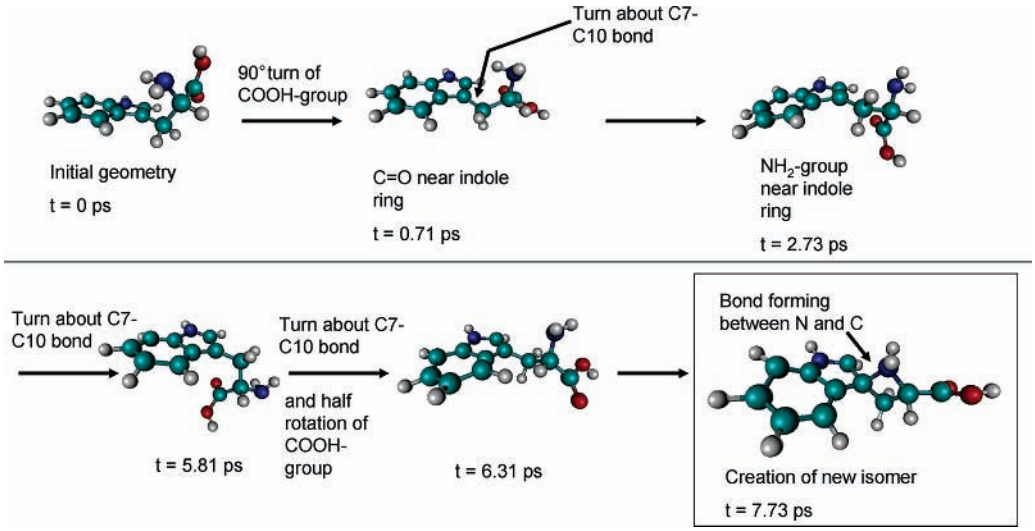

Figure 7. Snapshots of the one-photon ionization dynamics of tryptophan: creation of new isomer.

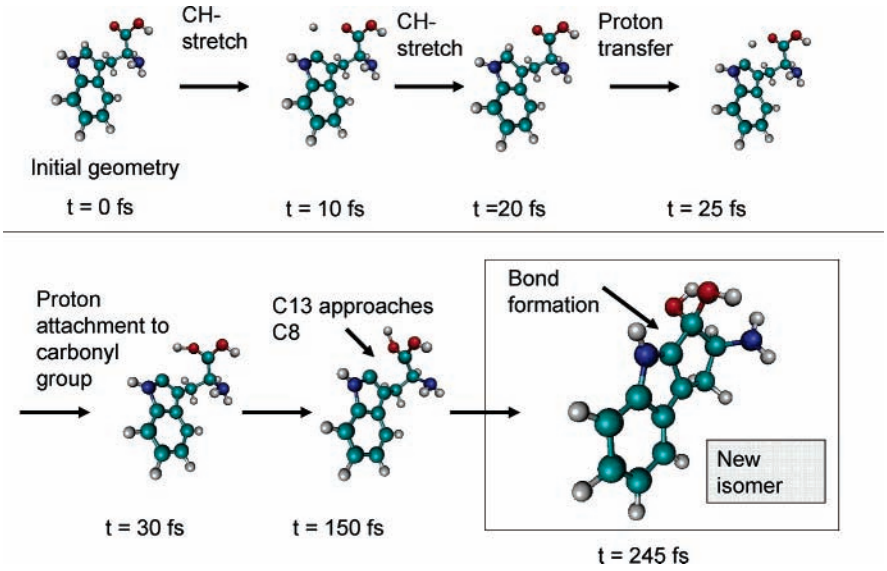

Figure 8. Snapshots of the one-photon ionization dynamics of tryptophan: creation of new isomer.

ps. Minor changes have also occurred in this time span, such as, for example, rotation of the hydroxyl group. The nitrogen of the amino group comes closer to the indole ring. At $t = 7.73$ ps a new isomer is formed. This isomer remains stable until the end of the simulation (10 ps). This isomer was optimized with PM3 and found to be a minimum (all frequencies are positive). This isomer has also been optimized with second-order Møller−Plesset perturbation theory (MP2) with a double-ζ polarization (DZP) basis set. The calculation found an optimized structure. To our knowledge, this structure is unknown in the literature.

Another trajectory shows the creation of another new isomer. In this trajectory, the CH-stretch mode (frequency: 3085.02 cm^{-1}) of the indole ring (see Figure 8) is initially distorted to −33.738 34 au. The excess energy for this trajectory is 6.5 eV. Figure 8 shows the dynamics. Initially, there is one CH stretch. The proton then detaches again and jumps to the carbonyl group at 30 fs. Carbon C13 then approaches the indole ring and creates a bond with C8 at 245 fs. This conformer remains stable until the end of the simulation (10 ps). This isomer was optimized with PM3 and found to be a minimum (all frequencies were positive). This isomer has also been optimized with MP2 with a DZP basis set. All frequencies are positive. The calculation found an optimized structure. To our knowledge, this structure is also not known in the literature.

All the events described above happen in trajectories with relatively high excess energy. This excess energy enables the fast hydrogen/proton hopping and the creation of new isomers.

(c) Energy Flow between the Indole Ring and the Amino Acid Backbone. Figure 9 shows the energy flow between the amino acid backbone and the ring modes. The same method as before of effective temperatures has been used. Initially, the amino acid backbone modes are much hotter than the ring modes. The ring modes only vibrate around the equilibrium configuration, whereas the amino acid backbone undergoes large structural changes. Equilibration to a common temperature is very fast (about 2 ps). Later on, there are again larger fluctuations in the temperature (see at $t \approx 8$ ps). It can be concluded that energy flow is very effective in the case of one-photon ionization. The effective temperature equilibrates in a short time, reaching the same value for the two groups.

IV. Conclusions

It has been shown that the two-photon ionization of tryptophan leads to fast conformational transitions in the ion formed.

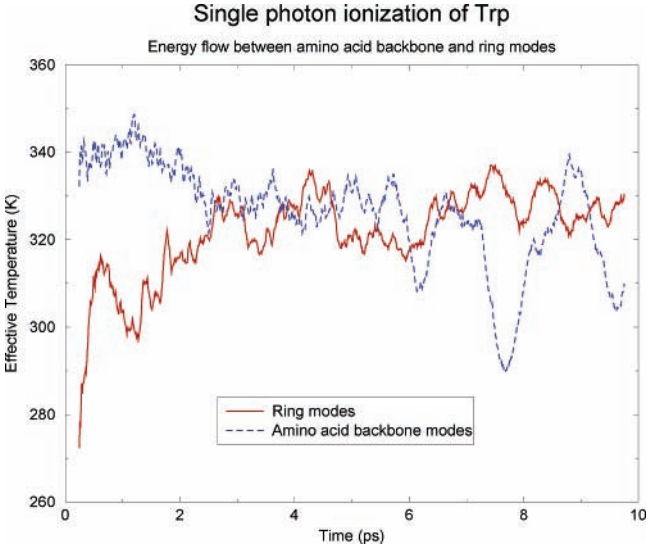

Figure 9. Effective temperature of the ring modes and the amino acid backbone modes of the one-photon ionization averaged over all trajectories up to 10 ps.

Two conformers are pointed out that are especially stable and occur in many trajectories. No isomerization is observed in the case of the two-photon ionization. One-photon ionization also shows the same conformers as described in the two-photon ionization. But, additionally, there are two new isomers created during the dynamics, which are the first time reported here. Also, in two trajectories, proton transfer from the carboxyl group to the amino group and back is observed. This yields a zwitterion. This zwitterion is not stable, because the proton is transferred back very fast. Energy flow in all cases studied here is very extensive. Partial equilibration is reached very fast, but it seems that it is not complete over the time scale studied. The richness of conformation transitions, proton-transfer processes and intramolecular vibrational energy flow processes observed in this simulations for ultrafast time scales suggest the desirability of ultrafast experiments to verify these events and determine their role in mass spectrometry of such molecules.

Acknowledgment. This paper is dedicated to the memory of Chava Lifshitz, a highly appreciated colleague, a friend and a teacher. We have learned enormously from her unique knowledge of the field. Her insight will continue to impact our work in the future.

References and Notes

(1) Yamashita, M.; Fenn, J. B. *J. Phys. Chem.* **1984**, *88* (20), 4451.
(2) Yamashita, M.; Fenn, J. B. *J. Phys. Chem.* **1984**, *88* (20), 4671.
(3) Alexandrov, M. L.; Gall, L. N.; Krasnov, N. V.; Nikolaev, V. I.; Pavlenko, V. A.; Shkurov, V. A.; Baram, G. I.; Grachev, M. A.; Knorre, V. D.; Kusner, Y. S. *Bioorg. Khim.* **1984**, *10* (5), 710.
(4) Karas, M.; Bachmann, D.; Bahr, U.; Hillenkamp, F. *Int. J. Mass Spectrom. Ion Processes* **1987**, *78*, 53.
(5) Bowers, M. T.; Marshall, A. G.; McLafferty, F. W. *J. Phys. Chem.* **1996**, *100* (31), 12897.
(6) Burlingame, A. L.; Boyd, R. K.; Gaskell, S. J. *Anal. Chem.* **1998**, *70* (16), 647r.
(7) Chalmers, M. J.; Gaskell, S. J. *Curr. Opin. Biotechnol.* **2000**, *11* (4), 384.
(8) Aebersold, R.; Goodlett, D. R. *Chem. Rev.* **2001**, *101* (2), 269.
(9) Nyman, T. A. *Biomol. Eng.* **2001**, *18* (5), 221.
(10) Mann, M.; Hendrickson, R. C.; Pandey, A. *Annu. Rev. Biochem.* **2001**, *70*, 437.
(11) Griffiths, W. J.; Jonsson, A. P.; Liu, S. Y.; Rai, D. K.; Wang, Y. Q. *Biochem. J.* **2001**, *355*, 545.
(12) Jonsson, A. P. *Cellular Molecular Life Sci.* **2001**, *58* (7), 868.
(13) Mano, N.; Goto, J. *Anal. Sci.* **2003**, *19* (1), 3.
(14) Ferguson, P. L.; Smith, R. D. *Annu. Rev. Biophys. Biomol. Struct.* **2003**, *32*, 399.
(15) Lin, D.; Tabb, D. L.; Yates, J. R. *Biochim. Biophys. Acta—Proteins Proteom.* **2003**, *1646* (1−2), 1.
(16) Aebersold, R.; Mann, M. *Nature* **2003**, *422* (6928), 198.
(17) Standing, K. G. *Curr. Opin. Struct. Biol.* **2003**, *13* (5), 595.
(18) Koster, C.; Grotemeyer, J. *Org. Mass Spectrom.* **1992**, *27* (4), 463.
(19) Schlag, E. W.; Grotemeyer, J.; Levine, R. D. *Chem. Phys. Lett.* **1992**, *190* (6), 521.
(20) Lockyer, N. P.; Vickerman, J. C. *Int. J. Mass Spectrom.* **1998**, *176* (1−2), 77.
(21) Vorsa, V.; Kono, K.; Willey, F.; Winograd, N. *J. Phys. Chem. B* **1999**, *103* (37), 7889.
(22) Lockyer, N. P.; Vickerman, J. C. *Int. J. Mass Spectrom.* **2000**, *197*, 197.
(23) Cohen, R.; Brauer, B.; Nir, E.; Grace, L.; de Vries, M. S. *J. Phys. Chem. A* **2000**, *104* (27), 6351.
(24) Godfrey, P. D.; Brown, R. D. *J. Am. Chem. Soc.* **1995**, *117* (7), 2019.
(25) McGlone, S. J.; Elmes, P. S.; Brown, R. D.; Godfrey, P. D. *J. Mol. Struct.* **1999**, *486*, 225.
(26) Depke, G.; Heinrich, N.; Schwarz, H. *Int. J. Mass Spectrom. Ion Processes* **1984**, *62* (1), 99.
(27) Simon, S.; Sodupe, M.; Bertran, J. *J. Phys. Chem. A* **2002**, *106* (23), 5697.
(28) Rizzo, T. R.; Park, Y. D.; Levy, D. H. *J. Am. Chem. Soc.* **1985**, *107* (1), 277.
(29) Rizzo, T. R.; Park, Y. D.; Levy, D. H. *J. Chem. Phys.* **1986**, *85* (12), 6945.
(30) Rizzo, T. R.; Park, Y. D.; Peteanu, L.; Levy, D. H. *J. Chem. Phys.* **1985**, *83* (9), 4819.
(31) Rizzo, T. R.; Park, Y. D.; Peteanu, L. A.; Levy, D. H. *J. Chem. Phys.* **1986**, *84* (5), 2534.
(32) Elokhin, V. A.; Krutchinsky, A. N.; Ryabov, S. E. *Rapid Commun. Mass Spectrom.* **1991**, *5* (6), 257.
(33) Ayre, C. R.; Moro, L.; Becker, C. H. *Anal. Chem.* **1994**, *66* (10), 1610.
(34) Dey, M.; Grotemeyer, J. *Org. Mass Spectrom.* **1994**, *29* (11), 659.
(35) Reilly, P. T. A.; Reilly, J. P. *Rapid Commun. Mass Spectrom.* **1994**, *8* (9), 731.
(36) Belov, M. E.; Alimpiev, S. S.; Mlynsky, V. V.; Nikiforov, S. M.; Derrick, P. J. *Rapid Commun. Mass Spectrom.* **1995**, *9* (14), 1431.
(37) Callis, P. *Methods Enzymol.* **1997**, *278*, 113.
(38) Lindinger, A.; Toennies, J. P.; Vilesov, A. F. *J. Chem. Phys.* **1999**, *110* (3), 1429.
(39) Kushwaha, P. S.; Mishra, P. C. *J. Photochem. Photobiol. A—Chem.* **2000**, *137* (2−3), 79.
(40) Piuzzi, F.; Dimicoli, I.; Mons, M.; Tardivel, B.; Zhao, Q. C. *Chem. Phys. Lett.* **2000**, *320* (3−4), 282.
(41) Compagnon, I.; Hagemeister, F. C.; Antoine, R.; Rayane, D.; Broyer, M.; Dugourd, P.; Hudgins, R. R.; Jarrold, M. F. *J. Am. Chem. Soc.* **2001**, *123* (34), 8440.
(42) Snoek, L. C.; Kroemer, R. T.; Hockridge, M. R.; Simons, J. P. *Phys. Chem. Chem. Phys.* **2001**, *3* (10), 1819.
(43) Bakker, J. M.; Aleese, L. M.; Meijer, G.; von Helden, G. *Phys. Rev. Lett.* **2003**, *91* (20).
(44) Huang, Z. J.; Lin, Z. J. *J. Phys. Chem. A* **2005**, *109* (11), 2656.
(45) Weiner, P. K.; Kollmann, P. A. *J. Comput. Chem.* **1981**, *2*, 287.
(46) Weiner, S. J.; Kollman, P. A.; Case, D. A.; Singh, U. C.; Ghio, C.; Alagona, G.; Profeta, S.; Weiner, P. *J. Am. Chem. Soc.* **1984**, *106* (3), 765.
(47) Jorgensen, W. L.; Maxwell, D. S.; TiradoRives, J. *J. Am. Chem. Soc.* **1996**, *118* (45), 11225.
(48) Jorgensen, W. L.; Tiradorives, J. *J. Am. Chem. Soc.* **1988**, *110* (6), 1657.
(49) Halgren, T. A. *J. Comput. Chem.* **1996**, *17* (5−6), 490.
(50) Halgren, T. A. *J. Comput. Chem.* **1996**, *17* (5−6), 553.
(51) Stewart, J. J. P. *J. Comput. Chem.* **1989**, *10* (2), 209.
(52) Stewart, J. J. P. *J. Comput. Chem.* **1989**, *10* (2), 221.
(53) Jensen, F. *Introduction to Computational Chemistry*; Wiley and Sons: Chichester, U.K., 1999.
(54) Stewart, J. J. P. *J. Mol. Struct. (THEOCHEM)* **1997**, *401* (3), 195.
(55) Lee, T. S.; York, D. M.; Yang, W. T. *J. Chem. Phys.* **1996**, *105* (7), 2744.
(56) Daniels, A. D.; Scuseria, G. E. *J. Chem. Phys.* **1999**, *110* (3), 1321.
(57) Brauer, B.; Chaban, G. M.; Gerber, R. B. *Phys. Chem. Chem. Phys.* **2004**, *6* (10), 2543.
(58) Jung, J. O.; Gerber, R. B. *J. Chem. Phys.* **1996**, *105* (23), 10332.
(59) Chaban, G. M.; Jung, J. O.; Gerber, R. B. *J. Chem. Phys.* **1999**, *111* (5), 1823.
(60) http://www.msg.ameslab.gov/GAMESS/GAMESS.html.
(61) Stewart, J. J. P.; Davis, L. P.; Burggraf, L. W. *J. Comput. Chem.* **1987**, *8* (8), 1117.
(62) Maluendes, S. A.; Dupuis, M. *J. Chem. Phys.* **1990**, *93* (8), 5902.

(63) Gordon, M. S.; Chaban, G.; Taketsugu, T. *J. Phys. Chem.* **1996**, *100* (28), 11512.
(64) Takata, I.; Taketsugu, T.; Hirao, K.; Gordon, M. S. *J. Chem. Phys.* **1998**, *109* (11), 4281.
(65) Taketsugu, T.; Gordon, M. S. *J. Chem. Phys.* **1995**, *103* (23), 10042.
(66) Taketsugu, T.; Gordon, M. S. *J. Phys. Chem.* **1995**, *99* (40), 14597.
(67) Taketsugu, T.; Gordon, M. S. *J. Phys. Chem.* **1995**, *99* (21), 8462.
(68) Wang, J. P.; Meroueh, S. O.; Wang, Y. F.; Hase, W. L. *Int. J. Mass Spectrom.* **2003**, *230* (1), 57.
(69) Wang, Y. F.; Hase, W. L. *J. Am. Soc. Mass Spectrom.* **2003**, *14* (12), 1402.
(70) Wigner, E. *Phys. Rev.* **1932**, *40*, 749.